



Universiteit
Leiden
The Netherlands

Exploring charge transport properties and functionality of molecule-nanoparticle ensembles

Devid, E.J.

Citation

Devid, E. J. (2015, December 17). *Exploring charge transport properties and functionality of molecule-nanoparticle ensembles*. *Casimir PhD Series*. Retrieved from <https://hdl.handle.net/1887/37091>

Version: Not Applicable (or Unknown)

License: [Leiden University Non-exclusive license](#)

Downloaded from: <https://hdl.handle.net/1887/37091>

Note: To cite this publication please use the final published version (if applicable).

Cover Page



Universiteit Leiden



The handle <http://hdl.handle.net/1887/37091> holds various files of this Leiden University dissertation.

Author: Devid, Edwin Johan

Title: Exploring charge transport properties and functionality of molecule-nanoparticle ensembles

Issue Date: 2015-12-17

1



Introduction to molecular charge transport

This chapter contains a brief introduction to the research field of molecular charge transport. First, I deal with its basic driving force and its interesting history. Next, the experimental state of the art is highlighted by introducing the main experimental methods used in present-day research. Then, I will introduce the research in this dissertation, which deals with the question if and how molecular properties can be transferred to or even enhanced in molecular devices. I will pay extra attention to a special type of functional molecules, exhibiting a temperature-dependent spin transition, since it forms a key inspiration for this work. The chapter ends with an outlook on the rest of this thesis. Basic theory on molecular charge transport will be given in Chapter 2.

1.1 The motivation behind molecular charge transport

Research on molecular charge transport is motivated by a simple, but fascinating concept: the idea that a functional device, e.g. a transistor, switch or diode, may be as small as a single molecule connected to electrodes. This concept offers two interconnected advantages. First of all, such devices would be much smaller than present-day silicon components, i.e. around a few nanometers in size (disregarding the electrodes, however). Second, functionalities, such as switchability, rectification, etc., may be pre-programmable in the molecules used. The question if a device incorporating a functional molecule retains the same functionality is generally open. In fact, in many cases, coupling of a molecule to electrodes leads to a dramatic change of properties. This issue has been the subject of considerable scientific efforts and is also touched upon in this dissertation. From a basic research point of view, molecular charge transport has also attracted much attention. This is because small organic molecules are profoundly quantum mechanical in nature, even at elevated temperatures. Hence, the wave nature of the electron as well as its spin degree of freedom should be explicitly considered.

All the ingredients above have motivated scientists from various backgrounds to investigate the properties of molecular devices over the past decades. Chemists, physicists and surface scientists have joined hands, leading to considerable cross-fertilization. Especially with the rise of scanning probe microscopy as well as nanolithography techniques, the field of molecular charge transport (and nanoscience as a whole) seriously took off. During its history that spans around four decades now, it has both seen fast progress and backdrops [1]. For example, few people still believe that molecular electronics will be seriously competitive with silicon electronics. Still, the research has continued to prove fundamentally fascinating, while specific applications, e.g. as sensors, are being explored [2].

1.1.1 A short history of molecular charge transport

The conception of this research field lies between 1950 and 1960, i.e. the time of the invention of the transistor, an era that changed electronics completely. Since 1960, the quest to miniaturize electronic components has continued via a top-down approach (as analyzed by G. E. Moore) [3]. The miniaturization of silicon based electronics was ongoing and successful, but this also brought more complexity and high investment costs. Already then, some people feared that the miniaturization of silicon-based

electronics was bound to arrive at a technological dead end. Hence, the search started toward radically different alternatives to miniaturize electronics.

One way was to miniaturize electronic components via a bottom-up approach. This idea was formulated by A. von Hippel and it was then called molecular engineering [4]. This concept led, at the end of the 1950's, to the name "molecular electronics". This name embodied a new strategy between collaborating research institutes and USA defense-affiliated research branches to fabricate miniaturized electrical components. However, this concept could not compete with the steady miniaturization of the electronic devices from the semiconductor industry. Silicon-based electronic devices evolved further becoming smaller, lighter, consuming less power and emitting less heat [5].

Whereas in the 50's, molecular electronics strived to make microelectronics based on the use of crystalline bulk materials [5], in the 1970's, the perspective shifted to the use of individual molecules as electronic circuits. This was partially inspired by the famous speech by Richard Feynman called: "There's Plenty of Room at the Bottom", delivered in December 1959 [6]. The Swiss chemist H. Kuhn was one of the first scientists to experimentally explore the conductance properties of molecular monolayers. The latter were made by the Langmuir Blodgett method, i.e. via self-assembly of organic material floating on a liquid. B. Mann and H. Kuhn studied the transport of charge through both a "molecular" monolayer and "sandwiched" layers, made of fatty acid salts between metal electrodes [7]. Around the same period, A. Aviram and M. Ratner suggested to synthesize a new type of asymmetric molecular species. Once contacted by electrodes, it would be capable of rectification, thus mimicking the properties of semiconductor diodes in an electrical circuit [8]. Many experiments were conducted to realize this first type of a functional molecular device, but they were largely unsuccessful. Nevertheless, the idea that a molecule could be designed and synthesized with a certain functionality, and that that functionality could subsequently be transferred to a molecular device has remained an essential concept in molecular electronics ever since the Aviram-Ratner paper.

In 1981, IBM invented the first type of experimental platform that was truly capable of visualizing and investigating surfaces on the atomic scale: the scanning tunneling microscope (STM). It also became a key tool to study the charge transport properties of single molecules, as will be detailed below [9, 10]. In the 1990's, another experimental

device, called the mechanically controlled break junction (MCBJ) became available. The MCBJ was first used to study charge transport through metallic atomic-made wires [11], but was subsequently applied to molecular conductance studies as well [12].

At the end of the 90's, more experimental devices and fabrication techniques were introduced, some of which aimed for single molecular junctions, others which focused on probing molecular monolayers. The consequence was that also various companies became active in this field again [1]. The end of the 1990's hence saw a strong momentum, with various exciting results. Unfortunately, a few years later, some of the most spectacular results were heavily debated in literature. For example, HP labs aimed for a voltage-controlled molecular switch based on so-called rotaxanes molecules. These molecules are bistable switches in solution that can be controlled via a redox potential. An architecture of rotaxanes molecules circuits could indeed be made, for which memory/logic functions were demonstrated [13]. However, the interpretation of the achieved results was doubted by some researchers in the molecular charge transport community [14, 15]. The difficulty was that it was not at all clear if the switching effect observed was due to the molecules at all. Other explanations, such as metallic filament formation between the electrodes were (at least) equally probable [15]. This and other controversial situations disappointed scientists involved, and stalled the field for a few years. Fortunately, molecular charge transport as a basic research field picked up momentum again in the 2000's, in a more robust and perhaps also more modest way.

All in all, this brief history points out two of the key questions that will always arise in molecular charge transport: "Are the properties measured due to the contacted molecule?" And if so: "How is the molecule oriented within the device?". Rather fundamentally, these questions are not easy to answer. However, in this last decade, scientists have realized how to come close. Clearly, one wants additional control experiments, e.g. optical spectroscopy, Raman spectroscopy, inelastic electron tunneling spectroscopy (IETS). Furthermore, proper statistics of molecular junction formation and junction properties turn out to be of great importance. Through joint collaboration of researchers from various disciplines, creative methods have been devised that allow the study of the molecular charge transport properties in more robust types of molecular devices. Those molecular devices have the best chance of awaiting an application destiny in the future.

1.1.2 The role of organic molecules and their functionality

Conjugated organic molecules form the backbone of a large part of research on molecular junctions. A conjugated molecule typically contains an alternation of single and double (triple) carbon bonds. This yields an extended π -electron system, with orbitals composed of hybridized atomic p_z states. Conjugated molecules are expected to have relatively low resistance (but still higher than the quantum of resistance $h/2e^2 = 12.9 \text{ k}\Omega$!). Intuitively, this is due to two connected reasons. First, the π -orbitals are delocalized over the entire molecule, facilitating transport over the full entity. Second, the energy gap that separates the highest occupied molecular orbital (HOMO) from the lower unoccupied molecular orbital (LUMO) is lower than for non-conjugated systems, such as alkanes. In general, conjugated molecules will therefore have a larger conductance than non-conjugated molecules. Hence, much fundamental research is being performed on (series) of conjugated molecules. Clearly, this also opens an exciting possibility, i.e. to devise a molecule for which conjugation, and hence conductance, can be turned ‘on’ or ‘off’. As mentioned above, a prime motivation to investigate molecular charge transport has indeed been to study (and utilize) the role of molecular functionality. A molecular species can in principle be “programmed” to perform a certain function in a device. Chemical synthesis offers many ways to design and tailor the properties of organic molecules. For example, certain types of asymmetric molecules may lead to rectification behaviour, once the molecule is contacted (c.f. Aviram and Ratner [8]). Furthermore, a whole library of switchable molecules can be found in chemistry, some sensitive to light, others to temperature or electrochemical potential. The main molecular property that changes upon stimulation may vary. For some, conjugation is broken, others exhibit a length change (due to a cis-trans transformation), while a relatively unexplored subgroup exhibits a change of spin state. The latter type is of special interest for this thesis and will be dealt with in detail below.

As illustrated in the historical overview, a key question must be answered when investigating functional molecules in molecular junctions: “Is the functionality (and connected properties) preserved after a functional molecule is coupled to metal electrodes?” The answer is non-trivial and will depend on the details of the junction, i.e. (i) on the electrode material used, (ii) on the chemical group connecting the molecule to the electrodes and (iii) on the final geometry of the molecule with respect to the electrodes and other molecules [16]. Fundamentally, the molecular orbital structure

will change after connecting to electrodes, via hybridization between molecular orbitals and the metal bands, leading to broadened molecular levels (Lorentzians instead of delta functions, see Chapter 2). This is the case for any molecule, but for functional molecules it is of specific importance. A change in orbital structure may change the switching paths and dynamics completely. Clearly, the exact molecular endgroup that anchors the molecule to a metal surface also plays a key role in defining the exact electronic coupling. A general type of anchoring group used in organic molecules is a thiol (SH) group. The thiol group makes a chemical bond with gold and is the endgroup of choice in this work [1]. Finally, the detailed geometry and environment play a role if the switching process demands some free space available. Switching may be spatially hampered due to neighbouring atoms, molecules or electrodes. Chemists tend to refer to this as ‘steric hindrance’.

To illustrate the above, let us consider a well-known family of switchable molecules, i.e., the diarylethenes. These molecules can be switched between a less conductive (broken conjugated) state and a more conductive (conjugated) state through exposure by different wavelengths of light. In solution, diarylethenes can be converted reversibly [17]. But when these diarylethenes are coupled to gold electrodes through thiol bonding, things change. For example, the molecule shown in Figure 1.1 can only switch in one direction after being contacted: from the ‘on’ state to the ‘off’ state. From that point the functional molecule loses functionality and it becomes passive. The loss of functionality is in this case most likely caused by strong electronic coupling of the diarylethene molecule with the metal. Indeed, by slight changes in the molecular endgroup (meta-coupled phenyls instead of thiophene rings), reversible switching could be recovered in a junction geometry [16]. This illustrates how subtle the issue of retaining molecular functionality can be.

Interestingly, one may also wonder if the presence of electrodes can lead to new functionality. Indeed, this may be the case, as the electrodes define new boundary conditions (i.e. break rotational symmetry that molecules do have in solution).

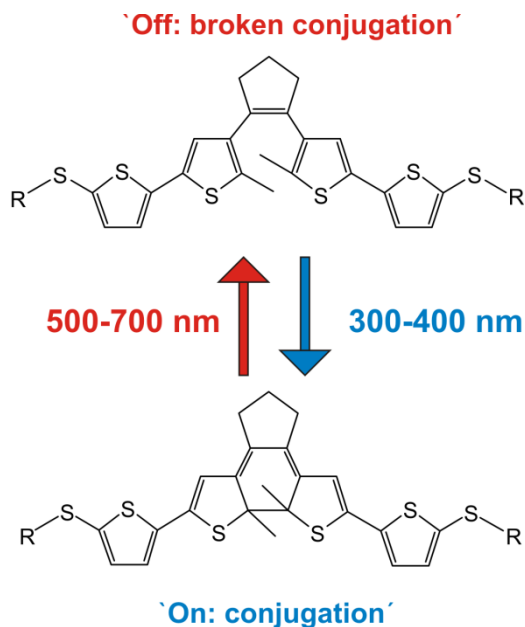


Figure 1.1: Example of a photochromic molecular switch that preserves intrinsic functionality in a solvent environment, but loses reversibility when coupled to metal electrodes.

Hence, the state in which the molecule is oriented parallel to the electrodes may have different properties than the state in which it is perpendicular. If one can switch between both situations, e.g. by a current or voltage, a switchable system is created. This is called extrinsic switching (as opposed to intrinsic switching which is due to the molecular properties themselves), and there are several experimental accounts for the phenomenon by now [16]. Another way in which the electrodes could play a role is in somehow enhancing the switching effect, e.g. by magnifying the conductance change. This thesis will also explore this possibility (see Chapter 4).

1.2 Experimental methods to study molecular conduction

A large set of experimental techniques is available nowadays to study charge transport through a single molecular junction or a multi-molecular junction. We will deal with the main techniques below, before presenting our method of choice that lies in between single molecular junctions and multi-molecular junctions.

1.2.1 Single molecular junctions

STM

Scanning tunneling microscopy (STM) is arguably the most widely used and versatile technique in the research on molecular charge transport. The STM serves a key role in measuring the charge transport properties of single molecular junctions [18, 19, 20] and recently also molecular chain junctions, by applying it unconventionally [21].

A standard STM consists of an atomically sharp metal tip placed above a surface (usually a metal substrate or a metal substrate covered by a very thin insulating layer) at a certain distance, d . During a STM measurement, a bias is applied between the tip and the metal electrode surface. The tip scans the surface of the sample, while its tunneling current is stabilized by a feedback circuit. In this way, STM can reach subatomic resolution. Hence, molecules lying on a surface can be imaged and spectroscopically investigated [1, 22-24]. For a true conductance experiment, however, the STM is used in a different fashion. Basically, the tip is connected to one end of a molecule connected to a surface. Next, the tip is raised (with the feedback mode off) and the conductance is tracked, until the newly formed junction breaks. When done at low temperature, in ultrahigh vacuum (UHV), this yields very good control over particular junctions. In somewhat adapted form, the method is also used at room temperature, to measure junction formation statistics and conductance properties of molecules in solution [25, 26].

The strong points of the STM lie in its versatility to perform both surface scans (and spectroscopy) and transport measurements. A weaker point is that its stability is limited compared to another experimental technique called mechanically controllable break junctions (see below). Also for the STM, which ideally is a single-molecule technique, charge transport measurements of long molecules (like alkanethiol molecules with a length of ~14 carbon atoms) become difficult as these yield very low currents only [27].

Mechanically controllable break junctions (MCBJ)

The term ‘break junction’ refers to an experimental technique in which a junction can be made by breaking one metal wire. When done properly, this results in two nearly symmetrical electrodes. There are two types of break junctions commonly used in the

field of molecular electronics, namely the electromigration break junctions (EBJ) and the mechanically controllable break junctions (MCBJ) [19].

The MCBJ was developed and used by J. Moreland [28] and J. M. van Ruitenbeek [29]. The platform consists of an insulating bendable substrate onto which a metal notched wire (or a lithographically defined metal bridge) is horizontally attached. The insulating substrate will be subjected to a tensile force in the z-direction under nanometer precision through a piezo controlled pushing rod. The counter supports on top of both sides of substrate assure that the sample remains fixed during bending. Upon bending, the substrate will elongate in the middle section of the notched electrodes. This finally causes the metal bridge to break. Once the junction has broken, molecules can be deposited on both fresh nanoscale electrodes. Due to a significant attenuation factor, the gap of the symmetric junction can be controlled below the Angstrom scale [30, 31], until ideally a single molecule can fit. This experimental technique was originally used by J. M. van Ruitenbeek to study atomic contacts and wires. Later, Müller brought the method to Reed's group and together they performed the first MCBJ study of a single molecule, i.e. a 1,4-benzenedithiol [32]. Nowadays, the MCBJ technique, like the STM technique described above, is used by many groups, both in low-temperature UHV experiments and for room-temperature measurements in solution.

The strong point of the MCBJ is that the distance between the metal electrodes can continuously be controlled via the piezo pushing rod. Furthermore, the MCBJ possesses a great stability, especially when working at low temperatures. In addition, with a MCBJ, one is able to repeatedly bend back and forth. This allows one to acquire a large number of measurements on which statistics can be performed [19]. A weaker point of the MCBJ is that one cannot take a topography scan of a single molecule, like in STM [1]. Connected, the exact shape of the metal contacts remains largely unknown.

Electromigration break junctions (EBJ)

A second experimental technique based on break junctions is due to Park *et al.* [33] who devised electromigration break junctions (EBJ). An EBJ is made by passing a large current density through a gold nanowire, defined by electron-beam lithography and shadow evaporation [19]. The electrons will have a net momentum transfer on the gold atoms that cause the latter to migrate to the positive electrode. This

electromigration process is continued until signs of eventual breakage of the gold nanowire becomes visible. Before the wire finally breaks, the current drops drastically and atomic sized contacts may be formed for a rather short time span. If done properly, two clean metal electrode contacts can be formed that are separated by a distance of around 1-2 nm [33-36]. A desired type of molecule can be inserted in this empty nanoscale gap.

A strong point of the experimental technique EBJ is that you can easily make a molecular three-terminal device with it [34, 36], i.e. a device that contains two electrodes contacting the molecule (source and drain) as well as a third, gate electrode. This gate electrode can be used to shift the energy levels of the molecule that is bridging the gap.

A weak point of the EBJ is that the atomic-sized metal contacts, made by electromigration, are hard to close again, unlike in MCBJs. This limits the sheer number of experiments possible, leading to very limited statistics compared to MCBJ and STM methods. Also EBJ is an experimental technique that asks a lot of care and fine-tuning to enable workable EBJ devices. An active feedback system is needed to carefully control the speed of the electromigration procedure [37]. If done incorrectly, metal debris can be formed in between the nearly symmetrically break junction during electromigration. The debris can hinder the insertion of molecules in between the break junction. Moreover, a small metal nanoparticle could have characteristics very similar to single molecules [38, 39].

1.2.2 Multi-molecular junctions

CP-AFM

An experimental technique that bears similarity to STM is conducting probe atomic force microscopy (CP-AFM) [19]. In contrast to STM, however, it is generally used for measurements on molecular monolayers. CP-AFM contains a metal-coated probe that can gently be positioned into contact with the molecules on a conducting surface. By applying a DC bias between the probe and the substrate, the charge transport properties of an ensemble of molecules on the conducting substrate surface can be measured [40-43]. An important difference between CP-AFM and STM is that in the first case, the force and deflection of the probe acting upon the molecules can be measured and controlled. In other words, there is an independent feedback mechanism, disconnected

from the conductance experiments themselves. Another advantage of (CP)-AFM is that the morphology of multi-molecular layers [44] till even polymer structures [45] can be determined while also their conductance can be probed. However, this experimental technique gives a higher uncertainty in the number of molecules measured, because a CP-AFM probe has a larger, often unknown, contact surface compared to an atomically sharpened STM tip. Furthermore, it requires a very sensitive control of the probe loading force [46].

Self-assembled monolayers (LAMJ configuration)

For technological applications, molecular tunnel junctions need to be reliable, reproducible and stable. In 2006, Akkerman *et al.* [47] introduced so-called large area molecular junctions (LAMJ), is also known as the “conductive polymer electrodes” technique [1]. The principle behind LAMJ is to create a self-assembled monolayer (SAM) on gold, onto which a conductive polymer layer is applied, followed by a gold top electrode. The polymer mixture used is poly[3,4-ethylenedioxythiophene] (PEDOT) : poly[4-styrenesulfonic acid] (PSS). It contains large hydrophilic macromolecules that cannot penetrate the hydrophobic densely packed SAM. Thus, the formation of short circuits by metal filaments from the top electrode will be prevented. The advantage of the LAMJ device is that the molecular junction is very robust [1]. The LAMJ device has a stability of at least a year in air, with no degradation of the SAM when sweeping the bias. Also the molecular ensemble of this LAMJ device can be analyzed by optical techniques. Finally, LAMJ devices can be fabricated within diameters up to $\sim 100 \mu\text{m}$ [47]. A weak point of such a LAMJ device, however, is that the shape of the current versus voltage, or $I(V)$, curves is partially determined by the PEDOT:PSS polymer. This makes LAMJ devices less favourable for fundamental research purposes.

1.3 Multi-molecular devices based on gold nanoparticles

An attractive method to study and explore charge transport through (functional) molecules is to make use of hybrid structures in which (gold) nanoparticles are connected by molecular bridges. The method, pioneered by Andres *et al.* [48] and explored by e.g. Schönberger and Jaeger [49-52] can be seen as a bridge between single-molecule and multi-molecular platforms. Its basic philosophy is to overcome the

long-standing problem of size mismatch between the molecules and the macroscopic electrodes by using an intermediate: (gold) nanoparticles ($\sim 10^{-8}$ m in diameter) connect between the nanoscopic (10^{-9} m) dimension of molecules and the macroscopic (10^{-7} to 10^{-3} m) dimensions of the metal electrodes (see Figure 1.2). This is done by connecting bottom-up approaches with top-down technology (lithography of the larger electrodes). Specifically, gold nanoparticles are first synthesized to the desired diameter (5-20 nm, typically). Next, they are covered by an alkanethiol shell, to prevent particle aggregation. Then, they are forced to assemble in a densely packed two-dimensional (2D) structure, on a water surface. The arrays thus formed are stamped on devices with pre-defined electrodes and can be investigated. A crucial step is yet to follow: molecular rods containing two thiol groups can be inserted between neighbouring nanoparticles. This so-called exchange step can take place spontaneously in a solution containing the molecular wires of interest. If a majority of the nanoparticle-molecule-nanoparticle junctions contain dithiolated molecular wires, these molecules will dominate the device's conductance properties.

Using molecule-metal nanoparticle arrays or networks (array will refer to a single layer; network to a few stacked molecule-nanoparticle ensembles) has various advantages. First of all, a large variety of molecular rods, including functional species, can be probed. Second, a conductance experiment will give a spatial average of single nanoparticle-molecule(s)-nanoparticle junctions probed both in series and in parallel. The sheet resistance of an array is ideally $R_{\square} = \frac{R_j}{\sqrt{3}} \approx 0.6R_j$, where R_j is the tunnel resistance of the molecule species in a nanoparticle junction [53]. Hence, results can be compared to time-dependent statistics as obtained in STM and MCBJ experiments. Third, the devices are relatively robust, lasting for between a week and a few months at room temperature. Due to the percolative nature of the devices, they are rather insensitive to defects. Finally, and perhaps most importantly, these networks allow for a range of control experiments. Whereas the signal from a single molecular junction is generally too small to be measurable by standard spectroscopic techniques, this is different for networks combining many junctions. As a result, optical spectroscopy, Raman spectroscopy, and even magnetization measurements come into play. This allows one to correlate (changes of) conductance properties to (changes of) molecular properties, thus relating directly to the key validation questions of the field, mentioned above.

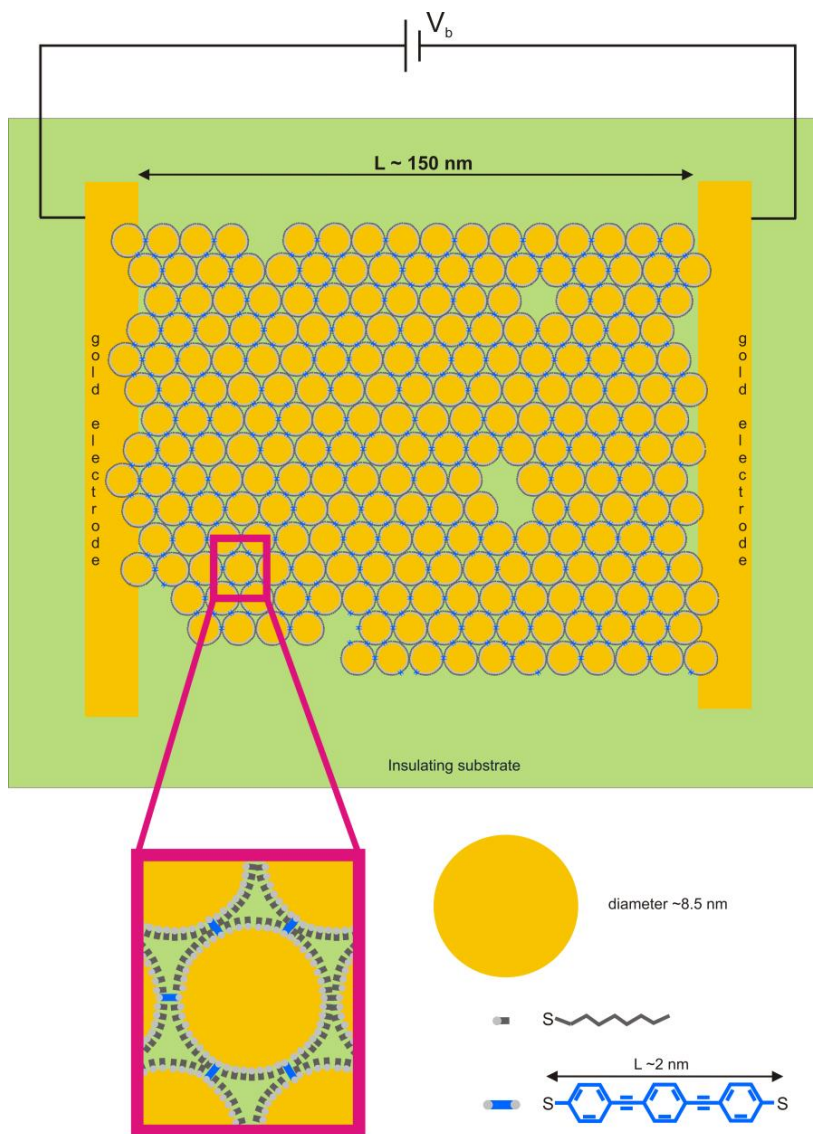


Figure 1.2: Schematic representation of a molecule-gold nanoparticle array deposited on a nanotrench device. The gold nanoparticles are encapsulated by octane(mono)thiol molecules (see gray coloured structure) to allow for self-assembly while avoiding aggregation and to tune the distance between the gold nanoparticles. Via molecular exchange, conjugated molecules (see e.g. the blue coloured bridge structure) can be inserted in between the gold nanoparticle junctions.

Vice versa, the open, 2D structure of molecule-gold nanoparticle arrays also permits molecular junctions to be addressed by external stimuli (i.e., light, pressure, magnetic field, temperature, etc.) [50, 54]. All of this makes the method very attractive to measure and benchmark (functional) molecules, specifically the spin transition molecules discussed below. Therefore, it is a key ingredient in the research presented here.

A weak point of a molecule-gold nanoparticle array connects directly to one of its advantages. At temperatures above ~ 360 K (roughly the experimental flashpoint of liquid octane(mono)thiol), the octanethiol molecules covering the nanoparticles start to decompose or detach. This leads to particle aggregation and eventually to device breakdown. When performing heating-cooling cycles, reversibility should therefore be checked. In Chapter 3, I will elaborate on this method and our work to extend it to three dimensions as well as to use different molecules to initially cover the nanoparticles, beyond alkanethiols. One of the main goals of this work, however, concerns interfacing and studying spin transition molecules in a device geometry. Next, I introduce this fascinating type of system.

1.4 Spin crossover molecules

A spin crossover (SCO) molecule is a molecule that can exhibit two different (total) spin states. Toggling between these configurations is possible via some external stimulus. This may be a temperature variation, irradiation by light or even a local electric field. Spin crossover systems have been synthesized and studied in bulk for over 80 years [55, 56]. Recently however, the research activity in this field has intensified. On the one hand, the prospect of applications has motivated chemists to increase the so-called transition temperature, the temperature at which the molecular system changes spin state, towards room temperature and above. For this, a set of ingeniously designed molecules have been synthesized [57, 58]. In parallel, there has been a trend towards nanoscopic length scales, down to the single molecules. Most of the chemical research is done on bulk powders of SCO molecules, where molecule-molecule interactions play a crucial role. Decreasing from macroscopic dimensions (bulk) down to the nanometer or even single-molecule scale could provide us with new understanding of the fundamentals of the spin transition properties. Devices based on spin transition molecules may find applications in nanoelectronics and spintronics, provided stability is somehow ensured. More generally, SCO molecules may serve as

promising molecular switches [59-62], image display [63], information storage [64, 65] and gas [66, 67] or temperature sensors [68].

However, the switching properties of SCO compounds may strongly differ at the nanoscale, as compared to bulk. In this thesis, specifically in Chapter 6, spin transition molecules will be investigated using nanoparticle networks. This allows us to measure conductance properties versus temperature, while also performing Raman spectroscopy and magnetization measurements. In the rest of this section, however, I will elaborate on the physics and chemistry behind SCO molecules. In general, these consists of a transition metal ion (e.g. Fe^{2+}) surrounded by organic ligands.

1.4.1 The metal complex

To understand what a spin crossover molecule is, we need to briefly review coordination chemistry. A coordination compound is a system in which a central metal ion is attached to a group of surrounding molecules or ions [69]. The organic molecules or ions that surround the central transition metal ion are called ligands. The ligands contain donor atoms that enable the formation of coordination bonds with the central transition metal ion. This means that both electrons involved in bond formation stem from the donor atom involved. Typically, coordination compounds need additional counterions (anions or cations) to acquire electrically neutrality. The term metal complex (or also complex) refers to both neutral coordination compounds and non-neutral coordination compounds.

The coordination number (CN) is the number of ligand donor atoms that surround the central transition metal ion in a complex. Depending on the nature of the central metal ion and its available number of p, d, or f orbitals, the coordination number can vary from 2 (linear), 4 (tetrahedral), 5 (pyramidal), 6 (octahedral) up to 12 (for lanthanides). Here I focus on the octahedral complexes, with CN equal to 6, which are typically found for d metal central ions, the so-called transition metals. For complexes based on transition metals, the distribution of the valence electrons in the available d orbitals is key to understanding their electronic, optical and magnetic behaviour. Different theoretical approaches can be used to understand the emergence of spin state switching.

1.4.2 Crystal and ligand field theory

We first use crystal field theory to explain the properties of a complex further. It is a model to describe how the coordination bonding in complexes arises from electrostatic interactions [70]. Here the coordination bonds are considered to have an “ionic” nature, i.e. there is an electrostatic attraction between the positively charged transition metal ion and the electronegative atoms of the ligands. The properties of a complex are described similarly to the properties of transition metal ions in ionic crystals.

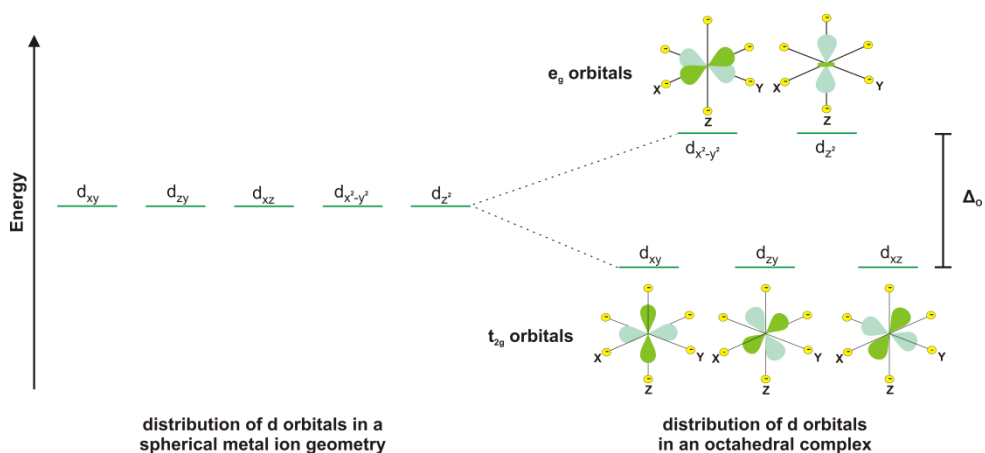


Figure 1.3: Schematic energy level diagram of the five degenerate d orbitals for a free ion (left) and in an octahedral complex (right), where the t_{2g} and e_g orbitals are split by a crystal field splitting energy Δ_o (see paragraph 1.4.2).

To understand crystal field theory of an octahedral complex, let us look at a d orbital energy level diagram (see Figure 1.3). For a metal ion in a spherically symmetric environment (such as in a free ion), there are five degenerate orbitals namely the d_{xy} , d_{xz} , d_{yz} , $d_{x^2-y^2}$ and d_z^2 . Now suppose the ligands are octahedrally closing in on a metal ion. Then the metal ion becomes subject to an electrical field from the charged atomic species on the ligand molecules. This crystal field disrupts the symmetry of a metal ion [71]. The d orbitals are repelled by the orbitals from the ligands and this gives changes in the energies of the five d orbitals. Three of the d orbitals, namely the d_{xy} , d_{xz} and d_{yz} , will adopt spatial orientations in between the charges oriented along the x, y, z axes of the ligands. The energies of these nonbonding d_{xy} , d_{xz} and d_{yz} orbitals (also called the

t_{2g} orbitals) will be lower compared to the other two antibonding d orbitals. These antibonding $d_{x^2-y^2}$ and d_z^2 orbitals (also called the e_g orbitals) will have direct repulsion with the charges of the ligand. The difference in energy between these two sets of d orbitals is called the crystal field splitting energy Δ_O . Depending on the metal ion and ligand species used to form a complex, different splitting energies arise [69, 70].

To find the spin state of a molecular complex, another competing energy scale is important: the mean spin pairing energy P . This is the energy it costs to pair two (interacting) electrons on one of the d orbitals. Now, let us consider a complex with an octahedral iron (Fe^{2+}) complex. Such a system can typically have one of two possible electron distributions of the six 3d valence electrons of the Fe^{2+} ion, corresponding to two different spin states [69, 70].

If $P \gg \Delta_O$, none of the d orbitals will be empty. One of the t_{2g} states will be doubly occupied, whereas the other four will contain one electron. Following the rules of Hund, these electrons will line up their spins. As a result, this complex will have spin quantum number $S = 2$ and it is said to be in a high-spin (HS) state (see Figure 1.4(a)) A high-spin Fe^{2+} complex behaves paramagnetically.

If $P \ll \Delta_O$, the six d-electrons of the Fe^{2+} will occupy the t_{2g} orbitals in three pairs. As a result, this complex has a total spin of $S = 0$. It is said to be in a low-spin (LS) state (see Figure 1.4(b)) and will behave like a diamagnetic complex.

We should note however, that Δ_O does not need to be the same for the molecule in its LS and HS states, somewhat complicating the picture above.

Crystal field theory is a simple and readily visualized ionic model to explain the electronic structure of complexes [70]. But crystal field theory is limited in that it only considers purely ionic bonds. Ligand field theory can be viewed as an extension of crystal field theory, combining concepts of the latter with features from molecular orbital theory. Ligand field theory incorporates the overlap between the ligand orbitals and the d orbitals of the metal ion. Also included is the delocalization of ligand and metal electrons in a complex. Nearly all the results of the crystal field theory are also valid in the ligand field theory [71].

Just like crystal field theory, ligand field theory takes into account the influence of electrostatic forces on the chemical bonding and origin of the orbital splitting of a complex. The presence of overlap will determine the ordering of the orbitals in

complexes and this scheme gives more understanding on Δ_o . To identify overlap, ligand orbitals need to be formulated into symmetrical adapted orbitals. These are then combined with the metal atomic orbitals to form molecular orbitals. Here the valence orbitals of both the ligand and metal ion are used to form symmetry adapted linear combinations (SALC). Based on empirical overlap and energy considerations an estimate can be made about the relative energies of a complex. These estimated energies will need further verification and adaptation before comparison can be made with experimental results [70].

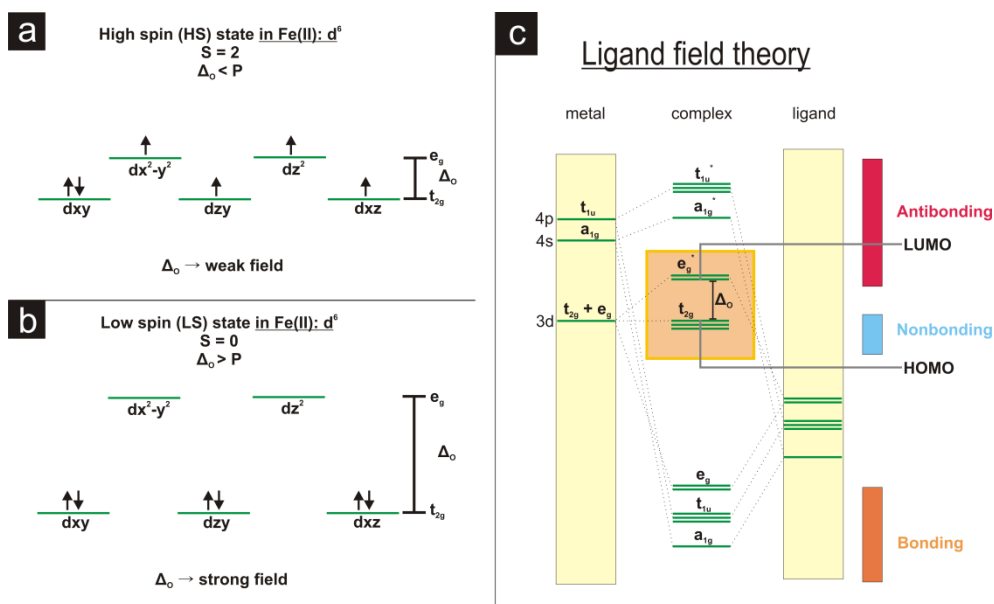


Figure 1.4: (a) Crystal field scheme of a Fe^{2+} complex in a high-spin (HS) configuration, possessing paramagnetic properties. (b) Crystal field scheme of a Fe^{2+} complex in a low-spin (LS) configuration, possessing diamagnetic properties. (c) Molecular orbital scheme of an octahedral complex according to ligand field theory (the * represents here the antibonding character). Ligand field theory allows to identify more accurately the origin and magnitude of the splitting energy Δ_o in a complex (see light orange box) compared to the crystal field theory. The ligand field theory scheme is based on σ bond overlap between the metal ion orbitals and the ligand orbitals.

From ligand field theory one learns that the molecular orbitals involved are partially confined to the metal atom. This is displayed in Figure 1.4(c), via a molecular orbital

energy level diagram. The ground-state electron configuration for a complex can be established through this diagram.

Two matters can be concluded from ligand field theory:

- The six bonding molecular orbitals are supplied by the ligands.
- The remaining n electrons of a d^n complex populate the nonbonding t_{2g} orbitals and the antibonding e_g orbitals. From that point, the crystal field theory approach is then followed.

If a ligand possesses π orbitals that may align with the σ bond along the metal-ligand axis of the complex, then both bonding and antibonding π molecular orbitals can be formed with the metal orbitals. The most crucial part of π bonding related to ligand field theory is that when ligand π orbitals are taken into account, overlap with the nonbonding t_{2g} orbitals can occur. The t_{2g} orbitals of the metal ion will become involved with the bonding of the complex and this will result into changes of the HOMO-LUMO gap [70]. Here, Δ_O can become larger or smaller, depending if the ligand species supplies π accepting orbitals or π donating orbitals, respectively. To inspect the role and influence of the ligand species with respect to Δ_O , a spectrochemical series can be constructed. This empirical ordering of ligands displays how strongly the π bonding will influence the Δ_O of a complex.

To summarize, according to ligand field theory both σ bonds and (possibly) π bonds occur in a complex. The type of ligand species influences, mainly via π bonding, the splitting energy Δ_O of a complex.

1.4.3 Spin crossover complexes

Spin crossover (SCO) molecules [55] (also called spin transition molecules [72]) are a special class of complexes that allow a transition between a low-spin (LS) and high-spin (HS) state. Typically, spin transition molecules will have $\Delta_O \approx P$, i.e. a spin transition can be described as a compromise between the correlative interactions (Hund's principle, energy scale P) and the ligand field energy scale [71]. The crossover is reached via a temperature increase (entropy driven) or by e.g. illumination.

For many decades, the iron (Fe^{2+}) ion has been the most studied metal ion in SCO bulk compounds [55, 58, 72, 73]. Also this thesis will focus on a SCO compound that contains an Fe^{2+} ion. Despite this long history, the synthesis of a Fe^{2+} SCO complex

that features a spin transition around room temperature is still both a science and an art [58].

In 2008, the research group of Mario Ruben developed a SCO molecule [72] by chemically tailoring a $[\text{Fe}(\text{AcS-BPP})_2](\text{ClO}_4)_2$ complex (where AcS-BPP denotes S-(4-{[2,6-(bipyrazol-1-yl)pyrid-4-yl]ethynyl}phenyl)ethanethioate). This metal complex is based on an iron (II) ion and two organic ligands (i.e. S-(4-{[2,6-(bipyrazol-1-yl)pyrid-4-yl]ethynyl}phenyl)ethanethioate). In Figure 1.5, the bulk powder form of this SCO complex is shown, denoted by the abbreviated formula $[\text{Fe}(\text{AcS-BPP})_2](\text{ClO}_4)_2$.

Note that the bulk $[\text{Fe}(\text{AcS-BPP})_2](\text{ClO}_4)_2$ complex contains protecting thioacetate groups to prevent oligomerization and polymerization of the bis-thiol anchoring groups on the bulk $[\text{Fe}(\text{AcS-BPP})_2](\text{ClO}_4)_2$ complex in a solution and allow access to form Au-S bonding between the gold nanoparticle and the complex [74]. After exposure to Au the bulk SCO molecule is deprotected and the composition of the SCO molecule becomes a $\text{Fe}^{2+}(\text{bis}(\text{pyrazol-1-yl})\text{pyridine})_2$ (i.e. $\text{Fe}(\text{S-BPP})_2$) complex. This $[\text{Fe}(\text{AcS-BPP})_2](\text{ClO}_4)_2$ complex can perform a spin transition via external stimuli such as temperature (T), light (λ), pressure (p) and magnetic field (H) [57, 72, 75]. In Figure 1.5 bottom, a magnetic susceptibility measurement of the bulk $[\text{Fe}(\text{AcS-BPP})_2](\text{ClO}_4)_2$ SCO compound is shown. This plot shows a rather abrupt spin transition, from a LS state at low temperatures to a HS state at high temperatures. Furthermore, it shows that the spin transition is reversible with limited thermal hysteresis. One can define $T_{1/2}$, i.e. the temperature where there is a 1:1 ratio of LS and HS molecules, when heated ($\uparrow T_{1/2}$) and cooled ($\downarrow T_{1/2}$). Both are close to room temperature for the $[\text{Fe}(\text{AcS-BPP})_2](\text{ClO}_4)_2$ complex in bulk, as $\downarrow T_{1/2} = 286$ K and $\uparrow T_{1/2} = 290$ K. During spin transition, a SCO molecule will undergo both an electronic change and a mechanical change. When going from the LS state to the HS state, the Fe-N bonds elongate a little and increase the molecular volume of the complex core. Hence, the total length of the $[\text{Fe}(\text{AcS-BPP})_2](\text{ClO}_4)_2$ SCO molecule can change slightly during a spin transition, as illustrated in Figure 1.5. Interestingly, hysteresis is very common in bulk SCO compounds. Moreover, it is seen as an important feature towards applications. Hysteresis is related to cooperativity, i.e. the ability to propagate the spin transition to neighbouring SCO molecules in a bulk SCO compound (i.e. solid crystal lattice). Via short- and long-range interactions a spin transition is elastically communicated to each SCO molecule (i.e. their metal core centres [76, 77]).

Fe(AcS-BPP)₂(ClO₄)₂ SCO complex

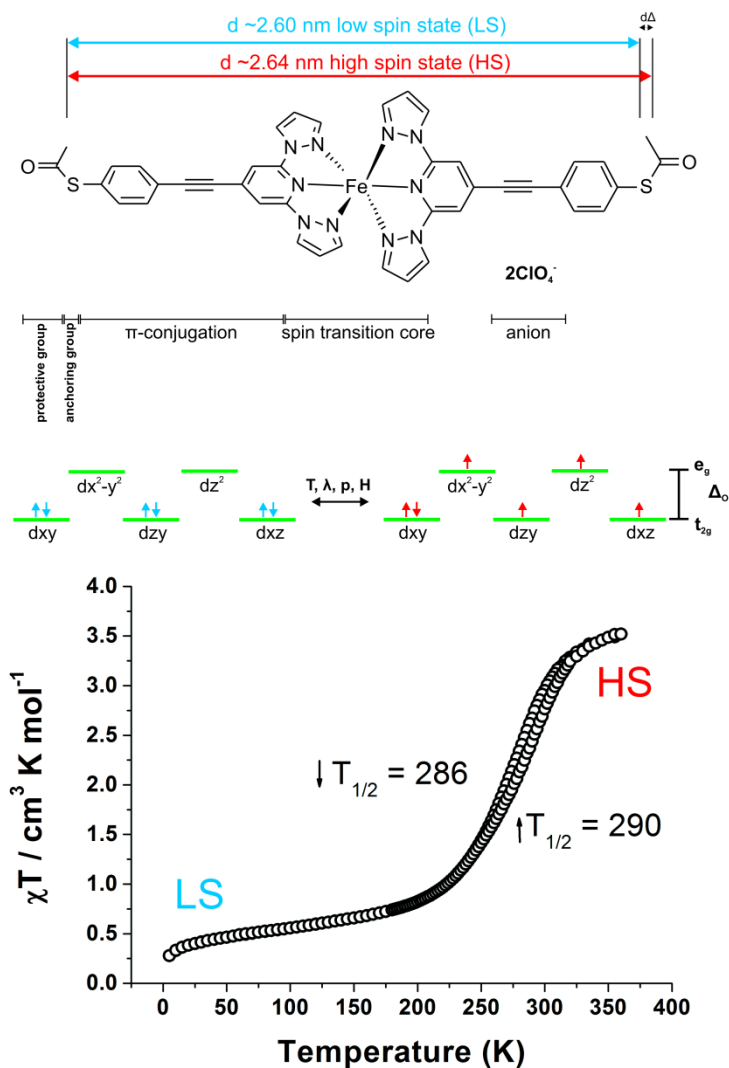


Figure 1.5: Room-temperature spin crossover $[\text{Fe}(\text{AcS-BPP})_2](\text{ClO}_4)_2$ complex. Top Figure shows the SCO molecular structure and its components. Except the electronic change also the molecular length (i.e. the spin transition core) of this complex changes very slightly during spin transition. Middle Figure shows a scheme of how the complex undergoes a spin transition. Bottom Figure shows a magnetic susceptibility plot of the bulk $[\text{Fe}(\text{AcS-BPP})_2](\text{ClO}_4)_2$ compound, indicating a reversible and stable spin transition with small thermal hysteresis, around the average transition temperature $T_{1/2} \approx 288 \text{ K}$.

A bulk SCO compound with low cooperativity, exhibits a gradual spin transition process. For a bulk SCO compound with high cooperativity, the spin transition can be more abrupt, i.e. take place within a very narrow range of temperature (~ 5 K), and thermal hysteresis can occur [55]. More generally, the transition between the LS and HS states can be abrupt, gradual, with or without hysteresis, follow a two-step transition or be incomplete [55]. In the next paragraph, we briefly go into the thermodynamics of the spin transition in bulk compound.

1.4.4 Spin transition in bulk

A spin transition can be modelled by a $x_{HS} = f(T)$ curve, where x_{HS} represents the molar fraction of HS molecular species [78]. For bulk SCO compounds this characteristic curve can be determined from magnetic measurements as function of temperature (i.e. $\chi T \propto f(T)$ plot, see Figure 1.5).

The stability of the two spin states (LS \leftrightarrow HS), is determined by the difference in Gibbs free energy (at constant pressure):

$$\Delta G = \Delta H - T\Delta S. \quad (1.1)$$

Here $\Delta G = G_{HS} - G_{LS}$. $\Delta H = H_{HS} - H_{LS}$ and $\Delta S = S_{HS} - S_{LS}$ denote the difference in enthalpy and entropy, respectively, for an assembly made of N molecules. At the temperature $T_{1/2}$ there is as much LS as HS present (disregarding hysteresis for now) so $\Delta G = 0$ and hence [78, 79]:

$$T_{1/2} = \frac{\Delta H}{\Delta S}. \quad (1.2)$$

The entropic term ΔS may be written as the sum of electronic ΔS_{el} and the vibrational ΔS_{vib} contributions:

$$\Delta S = \Delta S_{el} + S_{vib}, \quad (1.3)$$

where ΔS_{el} is related to the ratio of the electronic degeneracies g_{HS}/g_{LS} between the HS and LS states according to:

$$\Delta S_{el} = Nk_B \ln \left(\frac{g_{HS}}{g_{LS}} \right) [78]. \quad (1.4)$$

As for ΔS_{vib} , this is also positive and the vibrational disorder is more pronounced in the HS state, due to the longer metal-ligand bond lengths. In fact, ΔH and ΔS are both positive to have a finite and positive $T_{1/2}$.

A thermodynamic description of a spin transition is illustrated in Figure 1.6. At low temperatures T , the enthalpy term dominates and hence the LS state is the stable spin state species at 0 K. At the transition point, we have $G_{HS} = G_{LS}$ or $\Delta G = 0$ [78]. At high temperatures, above $T_{1/2}$, the entropic term will dominate, as shown in Figure 1.6(c). The HS state is the most stable spin state at elevated temperatures.

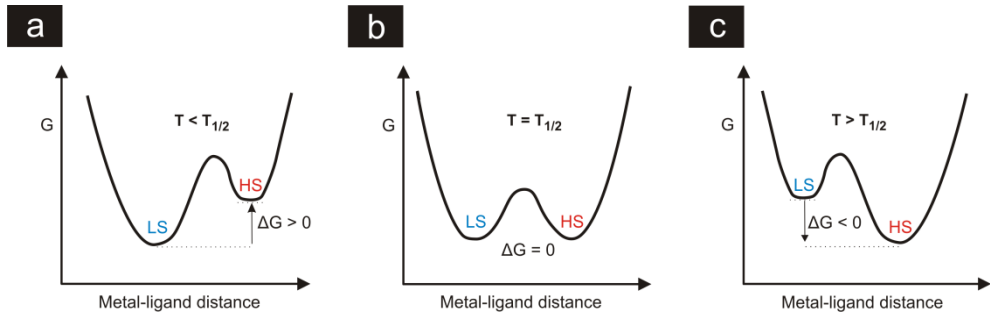


Figure 1.6. Schematic thermodynamic plots (Gibbs free energy (G) as a function of the metal-ligand distance) for a SCO bulk compound. The system changes from the LS (a) to the HS state or phase (c), as a function of temperature. At the spin transition temperature, $G_{HS} = G_{LS}$ (see (b)).

Even if there is no cooperativity, i.e. no direct intermolecular interaction in the SCO compound, one still needs to incorporate a mixing entropy term in the Gibbs free energy [78]. This mixing entropy S_{mix} represents the many ways to distribute $(x_{HS})N$ high-spin molecules and $(1-x_{HS})N$ low-spin molecules within the assembly of N molecules. It can be written as:

$$S_{mix} = -R[x_{HS} \ln(x_{HS}) + (1 - x_{HS}) \ln(1 - x_{HS})], \quad (1.5)$$

where R_B is the gas constant. Clearly, S_{mix} is maximum for $x_{HS} = 0.5$ and vanishes for $x_{HS} = 0$ and 1. The Gibbs free energy is then expressed as:

$$G = x_{HS}G_{HS} + (1 - x_{HS})G_{LS} - TS_{mix}. \quad (1.6)$$

The partial derivative of G with respect to x_{HS} gives:

$$\frac{\partial G}{\partial x} = \Delta G + RT \ln \left(\frac{x_{HS}}{1-x_{HS}} \right), \quad (1.7)$$

At any temperature and pressure, the equilibrium condition for the spin transition is defined by $\left(\frac{\partial G}{\partial x}\right)_{T,p} = 0$. Hence, we have

$$\ln \left(\frac{1-x_{HS}}{x_{HS}} \right) = \frac{\Delta G}{RT} = \frac{\Delta H}{RT} - \frac{\Delta S}{R}. \quad (1.8)$$

From which we obtain, incorporating equation 1.2:

$$x_{HS} = \frac{1}{1 + \exp \left[\frac{\Delta H}{R} \left(\frac{1}{T} - \frac{1}{T_{1/2}} \right) \right]}. \quad (1.9)$$

Equation 1.9 represents the basic macroscopic spin transition behaviour, i.e. $x_{HS} = f(T)$, of a SCO bulk compound without cooperativity. This simple theory is due to Slichter and Drickamer [80]. Note that within this model, the spin transition is never complete, even for $T \rightarrow \infty$.

1.4.5 Size effects on spin crossover molecules

It is largely an open question how the spin transition properties change when the size of a bulk SCO compound is reduced toward the nanoscale or even to single molecules. Recent studies have shown that the spin transition becomes smoother [81, 82]. Also the transition temperature can shift to lower values and hysteresis can become smaller or even vanish upon reducing the size of the SCO [81-84]. In general a decrease of the cooperativity should indeed be expected. Also the influence of a different physical-chemical environment around the nanoscale SCO needs to be considered [84]. SCO molecules are known to be sensitive to environmental conditions, such as packing, chemical and electrostatic conditions, the presence of solvent molecules, etc. [57, 75, 85-89]. Hence, for SCO complexes on the nanoscale, e.g. in molecular devices, the (research) question should be asked whether the spin transition remains and if so, if its properties change.

1.5 Motivation and outlook of this thesis

The research presented in this thesis has been performed within an European research project called INTERNET (i.e. INTERfacing single molecules via nanoparticle NETworks), funded by European Research Agency (ERA) via the NanoSci-E+ scheme.

Initially the project started with four research groups. Apart from our group at Leiden University, these were led by Bernard Doudin (Institut de Physique et Chimie des Matériaux de Strasbourg), Mario Ruben (Karlsruhe Institute of Technology) and Stefano Sanvito (Trinity College Dublin). Along the way, constructive partnerships with other research groups were formed as well, most notably with Tia Keyes (Dublin City University) and Christian Kübel (Karlsruhe Institute of Technology). The main objective of project INTERNET has been to realize and study the properties of a reliable molecular interface, specifically with the aim of investigating functional molecules. This dissertation reflects the research at Leiden and the measurements done in direct collaboration. For these, I travelled to Strasbourg, Karlsruhe and Dublin on many occasions.

Let me end this paragraph with a brief overview of the rest of this thesis.

In Chapter 2, a theoretical introduction is given in charge transport at the nanoscale and specifically in molecular junctions.

In Chapter 3, a closer look is taken at the experimental methods behind the self-assembly of molecule-gold nanoparticle arrays and networks. Furthermore several synthesis routes are explored to make new types of molecule-gold nanoparticle arrays. Besides introducing conductance experiments on these molecular devices, this chapter also describes several optical analysis methods, which can be used as control experiments. The possibility to combine several measurement techniques on one sample structure is a clear advantage of the approach taken.

In Chapter 4, the charge transport properties of gold nanoparticle networks functionalized by benchmark molecules (octanethiol molecules and conjugated dithiols) are investigated. At low temperatures, the gold nanoparticles in a molecule-gold nanoparticle network start to play their own role, displaying properties such as Coulomb blockade [90]. Charge transport becomes dominated by multiple inelastic cotunneling. By changing the molecular species in a molecule-gold nanoparticle network we study in which way the molecules themselves influence charge transport in this regime. Our work on passive molecules turns out to have an interesting consequence for molecular switches: the ratio of the on-state and off-state conductance values may be ‘artificially’ enhanced in a nanoparticle network [54].

In Chapter 5 we demonstrate the synthesis of a new type of molecule-gold nanoparticle array, where the gold nanoparticles are functionalized by S-BPP molecular species (the

half-molecules in Figure 1.5). We study the properties of these arrays, comparing them to alkanethiol-gold nanoparticle arrays.

Finally, in Chapter 6 we scrutinize the properties of $\text{Fe}(\text{S-BPP})_2$ SCO molecules in molecule-gold nanoparticle networks. We investigate if the spin functionality is preserved in such a structure and if so, how spin switching influences the conductance properties of such molecular devices.

1.6 References

1. J. C. Cuevas and E. Scheer, *Molecular Electronics: An Introduction to Theory and Experiment*, World Scientific, Singapore, **2010**.
2. S. J. van der Molen, R. Naaman, E. Scheer, J. B. Neaton, A. Nitzan, D. Natelson, N. J. Tao, H. S. J. van der Zant, M. Mayor, M. Ruben, M. Reed and M. Calame, Visions for a Molecular Future, *Nature nanotechnology*, **8**, (2013), 385-389.
3. G. E. Moore, Cramming More Components onto Integrated Circuits, *Electronics*, **38**, (1965), 114-117.
4. A. R. von Hippel, Molecular Engineering, *Science*, **123**, (1956), 315-317.
5. H. Choi and C. C. M. Mody, The Long History of Molecular Electronics: Microelectronics Origins of Nanotechnology, *Social Studies of Science*, **39**, (2009), 11-50.
6. R. P. Feynman, There's Plenty of Room at the Bottom, *Engineering and science*, **23**, (1960), 22-36.
7. B. Mann and H. Kuhn, Tunneling Through Fatty Acid Salt Monolayers, *J. Appl. Phys.* **42**, (1971), 4398-4405.
8. A. Aviram and M. Ratner, Molecular rectifiers, *Chem. Phys. Lett.*, **29**, 1974, 277-283.
9. G. Binnig, H. Rohrer, Ch. Gerber and E. Weibel, Vacuum Tunneling, *Physica B*, **109-110**, (1982), 2075-2077.
10. G. Binnig, H. Rohrer, Ch. Gerber and E. Weibel, Surface Studies by Scanning Tunneling Microscopy, *Phys. Rev. Lett.*, **49**, (1982), 57-61.
11. N. Agrait, A. L. Yeyati and J. M. van Ruitenbeek, Quantum properties of atomic-sized conductors, *Phys. Rep.*, **377**, (2003), 81-279.
12. M. A. Reed, C. Zhou, C. J. Muller, T. P. Burgin and J. M. Tour, Conductance of a Molecular Junction, *Science*, **278**, (1997), 252-254.
13. Y. Chen, G.-Y. Jung, D. A. A. Ohlberg, X. Li, D. R. Stewart, J. O. Jeppesen, K. A. Nielsen, J. F. Stoddart and R. S. Williams, Nanoscale Molecular-switch Crossbar Circuits, *Nanotechnology*, **14**, (2003), 462468.
14. J. R. Heath et al., E. A. Chandross and P. S. Weiss, More on Molecular Electronics, *Science*, **303**, (2004), 1136-1137.
15. R. F. Service, Next-generation Technology Hits an Early Midlife Crisis, *Science*, **302**, (2003), 556-559.

-
16. S. J. van der Molen and P. Liljeroth, Charge Transport Through Molecular Switches, *J. Phys.: Condens. Matter*, **22**, (2010), 133001(1-30).
 17. D. Dulić, S. J. van der Molen, T. Kudernac, H. T. Jonkman, J. J. D. de Jong, T. N. Bowden, J. van Esch, B. L. Feringa and B. J. van Wees, One-way Opto-electronic Switching of Photochromic Molecules on gold, *Phys. Rev. Lett.*, **91**, (2003), 207402(1-4).
 18. T. Miyamachi, M. Gruber, V. Davesne, M. Bowen, S. Boukari, L. Joly, F. Scheurer, G. Rogez, T. K. Yamada, P. Ohresser, E. Beaurepaire and W. Wulfhekel, Robust Spin Crossover and Memristance Across a Single Molecule, *Nat. Commun.*, **3**, (2012), 1-6.
 19. H. Song, M. A. Reed and T. Lee, Single Molecule Electronic Devices, *Adv. Mater.*, **23**, (2011), 1583-1608.
 20. R. Temirov, A. Lassise, F. B. Anders and F. S. Tautz, Kondo Effect by Controlled Cleavage of a Single-molecule Contact, *Nanotechnology*, **19**, (2008), 065401 (1-13).
 21. L. Lafferentz, F. Ample, H. Yu, S. Hecht, C. Joachim and L. Grill, Conductance of a Single Conjugated Polymer as a Continuous Function of its Length, *Science*, **323**, (2009), 1193-1197.
 22. M. F. Crommie, C. P. Lutz and D. M. Eigler, Imaging Standing Waves in a Two-dimensional Electron Gas, *Nature*, **363**, (1993), 524-527.
 23. J. Repp, G. Meyer, S. M. Stojkovic, A. Gourdon and C. Joachim, Molecules on Insulating Films: Scanning-tunneling Microscopy Imaging of Individual Molecular Orbitals, *Phys. Rev. Lett.*, **94**, (2005), 026803(1-4).
 24. H. C. Manoharan, C. P. Lutz and D. M. Eigler, Quantum Mirages Formed by Coherent Projection of Electronic Structure, *Nature*, **403**, (2000), 512-515.
 25. N. J. Tao, Electron Transport in Molecular Junctions, *Nature Nanotech.*, **1**, (2006), 173-181.
 26. L. Venkataraman, J. E. Klare, I. W. Tam, C. Nuckolls, M. S. Hybertsen and M. L. Steigerwald, Single-molecule Circuits with Well-defined Molecular Conductance, *Nano Letters*, **6**, (2006), 458-462.
 27. R. L. McCarley, D. J. Dunaway and R. J. Willicut, Mobility of the Alkanethiol-Gold (111) Interface Studied by Scanning Probe Microscopy, *Langmuir*, **9**, (1993), 2775-2777.
 28. J. Moreland and J. W. Ekin, Electron Tunneling Experiments Using NbSn "Break" Junctions, *J. Appl. Phys.*, **58**, (1985), 3888-3895.
 29. C. J. Muller, J. M. van Ruitenbeek and L. J. de Jongh, Conductance and Supercurrent Discontinuities in Atomic Scale Metallic Constrictions of Variable Width., *Phys. Rev. Lett.*, **69**, (1992), 140-143.
 30. N. Agrait, A. Levy Yeyati and J. M. van Ruitenbeek, Quantum Properties of Atomic-sized Conductors., *Physics Reports*, **377**, (2003), 81-279.
 31. S. A. G. Vrouwe, E. van der Giessen, S. J. van der Molen, D. Dulić and B. J. van Wees, Mechanics of Lithographically Defined Break Junctions, *Phys. Rev. B*, **71**, (2005), 035313(1-7).
 32. M. A. Reed, C. Zhou, C. J. Muller, T. P. Burgin and J. M. Tour, Conductance of a Molecular Junction, *Science*, **278**, (1997), 252-254.

33. H. Park, A. K. L. Lim, A. P. Alivisatos, J. Park and P. L. McEuen, Fabrication of Metallic Electrodes with Nanometer Separation by Electromigration, *Appl. Phys. Lett.*, **75**, (1999), 301-303.
34. J. Park, A. N. Pasupathy, J. I. Goldsmith, C. Chang, Y. Yaish, J. R. Petta, M. Rinkoski, J. P. Sethna, H. D. Abruña, P. L. McEuen and D. C. Ralph, Coulomb Blockade and the Kondo Effect in Single-atom Transistors, *Nature*, **417**, (2002), 722-725.
35. Y. Selzer, L. Cai, M. A. Cabassi, Y. Yao, J. M. Tour, T. S. Mayer and D. L. Allara, Effect of Local Environment on Molecular Conduction: Isolated Molecule versus Self-assembled Monolayer, *Nano Lett.*, **5**, (2005), 61-65.
36. W. J. Liang, M. P. Shores, M. Bockrath, J. R. Long and H. Park, Kondo Resonance in a Single-molecule Transistor, *Nature*, **417**, (2002), 725-729.
37. M. L. Trouwborst, S. J. van der Molen and B. J. van Wees, The Role of Joule Heating in the Formation of Nanogaps by Electromigration, *J. Appl. Phys.*, **99**, (2006), 114316(1-7).
38. H. B. Heersche, Z. de Groot, J. A. Folk, L. P. Kouwenhoven, H. S. J. van der Zant, A. A. Houck, J. Labaziewicz and I. L. Chuang, Kondo Effect in the Presence of Magnetic Impurities, *Phys. Rev. Lett.*, **96**, (2006), 017205(1-4).
39. A. A. Houck, J. Labaziewicz, E. K. Chan, J. A. Folk and I. L. Chuang, Kondo Effect in Electromigrated Gold Break Junctions, *Nano Lett.*, **5**, (2005), 1685-1688.
40. D. J. Wold and C. D. Frisbie, Formation of Metal-Molecule-Metal Tunnel Junctions: Microcontacts to Alkanethiol Monolayers with a Conducting AFM Tip, *J. Am. Chem. Soc.*, **122**, (2000), 2970-2971.
41. D. J. Wold and C. D. Frisbie, Fabrication and Characterization of Metal-Molecule-Metal Junctions by Conducting Probe Atomic Force Microscopy, *J. Am. Chem. Soc.*, **123**, (2001), 5549-5556.
42. J. M. Beebe, V. B. Engelkes, L. L. Miller and C. D. Frisbie, Contact Resistance in Metal-Molecule-Metal Junctions based on aliphatic SAMs: Effects of Surface Linker and Metal Work Function, *J. Am. Chem. Soc.*, **124**, (2002), 11268-11269.
43. G. Wang, T. W. Kim, G. Jo and T. Lee, Enhancement of Field Emission Transport by Molecular Tilt Configuration in Metal-Molecule-Metal Junctions, *J. Am. Chem. Soc.*, **131**, (2009), 5980-5985.
44. C. M. Guédon, H. Valkenier, T. Markussen, K. S. Thygesen, J. C. Hummelen, and S. J. van der Molen, Observation of Quantum Interference in Molecular Charge Transport, *Nature Nanotechnology*, **7**, (2012), 305-309.
45. D. B. Mitzi, L. L. Kosbar, C. E. Murray, M. Copel and A. Afzali, High-mobility Ultrathin Semiconducting Films prepared by Spin Coating, *Nature*, **428**, (2004), 299-303.
46. K.-A. Son, H. I. Kim and J. E. Houston, Role of Stress on Charge Transfer through Self-assembled Alkanethiol Monolayers on Au, *Phys. Rev. Lett.*, **86**, (2001), 5357-5360.
47. H. B. Akkerman, P. W. M. Blom, D. M. de Leeuw and B. de Boer, Towards Molecular Electronics with Large-area Molecular Junctions, *Nature*, **441**, (2006), 69-72.
48. R. P. Andres, J. D. Bielefeld, J. I. Henderson, D. B. Janes, V. R. Kolagunta, C. P. Kubiak, W. J. Mahoney and R. G. Osifchin, Self-assembly of a Two-dimensional

-
- Superlattice of Molecularly Linked Metal Clusters, *Science*, **273**, (1996), 1690-1693.
49. J. Liao, L. Bernard, M. Langer, C. Schönenberger and M. Calame, Reversible Formation of Molecular Junctions in 2D Nanoparticle Arrays, *Adv. Mater.*, **18**, (2006), 2444-2447.
50. L. Bernard, Y. Kamdzhilov, M. Calame, S. J. van der Molen, J. Liao and C. Schönenberger, Spectroscopy of Molecular Junction Obtained by Place Exchange in 2D Nanoparticle Arrays, *J. Phys. Chem. C*, **111**, (2007), 18445-18450.
51. X. M. Lin, H. M. Jaeger, C. M. Sorensen and K. J. Klabunde, Formation of Long-range-Ordered Nanocrystal Superlattices on Silicon Nitride Substrates, *J. Phys. Chem. B*, **105**, (2001), 3353-3357.
52. T. P. Bigioni, X. M. Lin, T. T. Nguyen, E. I. Corwin, T. A. Witten and H. M. Jaeger, Kinetically Driven Self Assembly of Highly Ordered Nanoparticle Monolayers, *Nature Materials*, **5**, (2006), 265-270.
53. C. M. Guédon, J. Zonneveld, H. Valkenier, J. C. Hummelen, S. J. van der Molen, Controlling the Interparticle Distance in a 2D Molecule-nanoparticle Network, *Nanotechnology*, **22**, (2011), 125205(1-5).
54. S. J. van der Molen, J. Liao, T. Kudernac, J. S. Agustsson, L. Bernard, M. Calame, B. J. van Wees, B. L. Feringa and C. Schönenberger, Light-controlled Conductance Switching of Ordered Metal-Molecule-Metal Devices, *Nano Letters*, **9**, (2009), 76-80.
55. P. Gütllich, Y. Garcia and H. A. Goodwin, Spin Crossover Phenomena in Fe(II) Complexes, *Chem. Soc. Rev.*, **29**, (2000), 419-427.
56. P. Gütllich and A. Hauser, Thermal and Light-induced Spin Crossover in Iron(II) Complexes, *Coord. Chem. Rev.*, **97**, (1990), 1-22.
57. M. Cavallini, I. Bergenti, S. Milita, J. C. Kengne, D. Gentili, G. Ruani, I. Šalitroš, V. Meded and M. Ruben, Thin Deposits and Patterning of Room-Temperature-Switchable One-dimensional Spin-crossover Compounds, *Langmuir*, **27**, (2011), 4076-4081.
58. Z. Arcis-Castillo, S. Zheng, M. A. Siegler, O. Roubeau, S. Bedoui and S. Bonnet, Tuning the Transition Temperature and Cooperativity of Bapbpy-based Mononuclear Spin-crossover Compounds: Interplay between Molecular and Crystal Engineering, *Chem. Eur. J.*, **17**, (2011), 14826-14836.
59. O. Kahn and C. Jay Martinez, Spin-transition Polymers: From Molecular Materials Toward Memory Devices, *Science*, **279**, (1998), 44-48.
60. J.-F. Létard, P. Guionneau and L. Goux-Capes, Towards Spin Crossover Applications, *Top. Curr. Chem.*, **235**, (2004), 221-249.
61. A. Bousseksou, G. Molnár and G. Matouzenko, Switching of Molecular Spin States in Inorganic Complexes by Temperature, Pressure, Magnetic Field and Light: Towards Molecular Devices, *Eur. J. Inorg. Chem.*, **2004**, (2004), 4353-4369.
62. P. Gamez, J. S. Costa, M. Quesada and G. Aromí, Iron Spin-crossover Compounds: From Fundamental Studies to Practical Applications, *Dalton Trans.*, **38**, (2009), 7845-7853.
63. J.-F. Létard, N. Daro and S. Auffret in *Spin Transition Materials*, patent US 2010/0178511, **2010**.

64. M. Cavallini, I. Bergenti, S. Milita, G. Ruani, I. Šalitraš, Z. R. Qu, R. Chandrasekar and M. Ruben, Micro- and Nanopatterning of Spin-transition Compounds into Logical Structures, *Angew. Chem.*, **120**, (2008), 8724-8728.
65. M. S. Alam, M. Stocker, K. Gieb, P. Müller, M. Haryono, K. Student and A. Grohmann, Spin-state Patterns in Surface-grafted Beads of Iron(II) Complexes, *Angew. Chem. Int. Ed.*, **49**, (2010), 1159-1163.
66. M. Ohba, K. Yoneda, G. Agustí, M. C. Muñoz, A. B. Gaspar, J. A. Real, M. Yamasaki, H. Ando, Y. Nakao, S. Sakaki and S. Kitagawa, Bidirectional Chemo-switching of Spin State in a Microporous Framework, *Angew. Chem.*, **121**, (2009), 4861-4865.
67. P. D. Southon, L. Liu, E. A. Fellows, D. J. Price, G. J. Halder, K. W. Chapman, B. Moubaraki, K. S. Murray, J. F. Létard and C. J. Kepert, Dynamic Interplay between Spin-crossover and Host-guest Function in a Nanoporous Metal-organic Framework Material, *J. Am. Chem. Soc.*, **131**, (2009), 10998-11009.
68. L. Salmon, G. Molnár, D. Zitouni, C. Quintero, C. Bergaud, J. C. Micheau and A. Bousseksou, A Novel Approach for Fluorescent Thermometry and Thermal Imaging Purposes Using Spin Crossover Nanoparticles, *J. Mater. Chem.*, **20**, (2010), 5499-5503.
69. J. McMurry and R. C. Fay, *Chemistry*, Prentice Hall, New Jersey, **2001**.
70. D. F. Shiver and P. W. Atkins, *Inorganic chemistry*, Oxford university press, Oxford, **1999**.
71. C. J. Ballhausen, *Introduction to ligand field theory*, McGraw-Hill, New York, **1962**.
72. R. Chandrasekar, F. Schramm, O. Fuhr and M. Ruben, An Iron(II) Spin-transition Compound with Thiol Anchoring Groups, *Eur. J. Inorg. Chem.*, **17**, (2008), 2649-2653.
73. S. Brooker and J. A. Kitchen, Nano-magnetic Materials: Spin Crossover Compounds vs. Single Molecule Magnets vs. Single Chain Magnets, *Dalton Trans.*, **36**, (2009), 7331-7340.
74. H. Valkenier, E. H. Huisman, P. A. van Hal, D. M. de Leeuw, R. C. Chiechi and J. C. Hummelen, Formation of High-quality Self-assembled Monolayers of Conjugated Dithiols on Gold: Base Matters, *J. Am. Chem. Soc.*, **133**, (2011), 4930-4939.
75. I. Šalitraš, O. Fuhr, A. Eichhöfer, R. Kruk, J. Pavlik, L. Dlháň, R. Boča and M. Ruben, The Interplay of Iron(II) Spin Transition and Polymorphism, *Dalton Trans.*, **41**, (2012), 5163-5171.
76. H. Spiering, T. Kohlhaas, H. Romstedt, A. Hauser, C. Bruns-Yilmaz, J. Kusz and P. Gütllich, Correlations of the Distribution of Spin States in Spin Crossover Compounds, *Coord. Chem. Rev.*, **192**, (1999), 629-647.
77. J. A. Real, A. B. Gaspar and M. C. Munoz, Thermal, Pressure and Light Switchable Spin-crossover Materials, *Dalton Trans.*, (2005), 2062-2079.
78. O. Kahn, *Molecular Magnetism*, VCH: New York, **1993**.
79. A. Bousseksou, J. J. McGarvey, F. Varret, J. A. Real, J.-P. Tuchagues, A. C. Dennis and M. L. Boillot, Raman Spectroscopy of the High- and Low-spin States of the Spin Crossover Complex Fe(phen)₂(NCS)₂: An Initial Approach to Estimation of Vibrational Contributions to the Associated Entropy Change, *Chemical Physics Letters*, **318**, (2000), 409-416.

-
80. C. P. Slichter and H. G. Drickamer, Pressure-induced Electronic Changes in Compounds of Iron, *J. Chem. Phys.*, **56**, (1972), 2142-2160.
81. M. Mikolasek, G. Félix, W. Nicolazzi, G. Molár, L. Salmon and A. Bousseksou, Finite Size Effects in Molecular Spin Crossover Materials, *New J. Chem.*, **38**, (2014), 1834-1839.
82. J. Larionova, L. Salmon, Y. Guari, A. Tokarev, K. Molvinger, G. Molár and A. Bousseksou, Towards the Ultimate Size Limit of the Memory Effect in Spin-crossover Solids, *Angew. Chem. Int. Ed.*, **47**, (2008), 8236-8240.
83. F. Volatron, L. Catala, E. Riviere, A. Gloter, O. Stephan and T. Mallah, Spin-crossover Coordination Nanoparticles, *Inorg. Chem.*, **47**, (2008), 6584-6586.
84. A. Bousseksou, G. Molnar, L. Salmon and W. Nicolazzi, Molecular Spin Crossover Phenomenon: Recent Achievements and Prospects, *Chem. Soc. Rev.*, **40**, (2011), 3313-3335.
85. S. Sanvito, Molecular Spintronics, *Chem. Soc. Rev.*, **40**, (2011), 3336-3355.
86. J. Olguin and S. Brooker, Spin Crossover Active Iron(II) Complexes of Selected Pyrazole-Pyridine Pyrazine Ligands, *Coordination Chemistry Reviews*, **255**, (2011), 203-240.
87. M. G. Cowan, J. Olguín, S. Narayanaswamy, J. L. Tallon and S. Brooker, Reversible Switching of a Cobalt Complex by Thermal, Pressure and Electrochemical Stimuli: Abrupt, Complete, Hysteretic Spin Crossover, *J. Am. Chem. Soc.*, **134**, (2012), 2892-2894.
88. M. Yamada, H. Hagiwara, H. Torigoe, N. Matsumoto, M. Kojima, F. Dahan, J.-P. Tuchagues, N. Re, and S. Iijima, A Variety of Spin-crossover Behaviours Depending on the Counter Anion: Two-dimensional Complexes Constructed by NH...Cl Hydrogen Bonds, $[\text{Fe}^{\text{II}}\text{H}_3\text{L}^{\text{Me}}]\text{Cl}\cdot\text{X}$ ($\text{X} = \text{PF}_6^-$, AsF_6^- , SbF_6^- , CF_3SO_3^- ; $\text{H}^3\text{L}^{\text{Me}} = \text{Tris}[2-\{[(2\text{-methylimidazol-4-yl)methylidene]amino\}ethyl]amine$), *Chem. Eur. J.*, **12**, (2006), 4536-4549.
89. I. Šalitroš, N. T. Madhu, R. Boča, J. Pavlik and M. Ruben, Room-temperature Spin-transition Iron Compounds, *Monatsh. Chem.*, **140**, (2009), 695-733.
90. M. A. Mangold, M. Calame, M. Mayor and A. W. Holleitner, Negative Differential Photoconductance in Gold Nanoparticle Arrays in the Coulomb Blockade Regime, *ACS Nano*, **6**, (2012), 4181-4189.

